Validation of GRACE/GRACE-FO Solutions Using Caspian Sea Level Change

Jianli Chen, Clark Wilson, Ki-Weon Seo, Anny Cazenave, Songyun Wang, Jin Li, and Yufeng Nie

***Abstract*—To validate gravity recovery and climate experiment (GRACE)/ GRACE follow-on (GRACE-FO) gravity solutions, we compare satellite altimetry observations of Caspian Sea level (CSL) change with CSL estimates from satellite gravity from April 2002 to December 2020. We use GRACE/GRACE-FO Release 6 GSM fields [spherical harmonics (SH)] from the three processing centers [Center for Space Research (CSR), Jet Propulsion Laboratory (JPL), and Geoscience Research Center (GFZ)] and three mascon solutions from CSR, JPL, and Goddard Space Flight Center (GSFC). CSL change is a regional scale signal that should be reasonably well resolved by satellite gravity measurements, but spatial leakage and other corrections are still required. We computed an average of smoothed SH solutions and those that are both smoothed and decorrelation filtered (to remove north–south stripe noise). Averaging mitigates attenuating effects of decorrelation filtering on the north–south oriented Caspian Sea Signal. After spatial leakage, terrestrial water storage, and steric corrections, most GRACE/GRACE-FO CSL estimates agree remarkably well with the altimetry series over a range of time scales as measured by trend and seasonal components and at other frequencies. The linear CSL trend from altimetry is -7.55 ± 0.17 cm/yr, while GRACE/GRACE-FO values range from -7.30 ± 0.17 to -8.66 ± 0.20 cm/yr. Annual amplitudes from altimetry are (17.75 ± 1.28 cm) with GRACE/GRACE-FO values in the range 17.05 ± 1.49 to 19.16 ± 1.55 cm, with good phase agreement. The GSFC mascon solution shows substantially smaller annual amplitude (11.62 ± 1.04 cm) than others. We found no bias between GRACE and GRACE-FO, but GRACE-FO shows larger root-mean-square differences from altimetry. Among the three standard SH solutions, those from CSR show the best agreement with altimetry.**

***Index Terms*—Caspian Sea level (CSL), GRACE/GRACE-FO, gravity, satellite altimeter, satellite gravimetry.**

Received 5 May 2024; revised 25 July 2024; accepted 19 August 2024. Date of publication 23 August 2024; date of current version 16 September 2024. This study was supported in part by the NSFC National Key Project under Grant 42394132, in part by Hong Kong RGC Collaborative Research Fund under Grant C5013-23G, and in part by NASA GRACE Follow-On Science Team Programs under Grant 80NSSC20K0820. *(Corresponding author: Jianli Chen.)*

Jianli Chen is with the Department of Land Surveying and Geo-Informatics, The Hong Kong Polytechnic University, Hong Kong, SAR, China, also with the Research Institute for Land and Space, The Hong Kong Polytechnic University, Hong Kong, SAR, China, and also with The Hong Kong Polytechnic University Shenzhen Research Institute, Shenzhen 518063, China (e-mail: jianli.chen@polyu.edu.hk).

Clark Wilson is with the Center for Space Research, University of Texas, Austin, TX 78712 USA, and also with the Department of Geological Sciences, Jackson School of Geosciences, University of Texas at Austin, Austin, TX 78712 USA (e-mail: crwilson@jsg.utexas.edu).

Ki-Weon Seo is with the Department of Earth Science Education, Seoul National University, Seoul 08826, South Korea (e-mail: seokiweon@snu.ac.kr).

Anny Cazenave is with the Toulouse University, LEGOS (CNES/CNRS/IRD/UT3), 31401 Toulouse, France (e-mail: anny.cazenave@univ-tlse3.fr).

Songyun Wang is with the Center for Space Research, University of Texas at Austin, Austin, TX 78712 USA (e-mail: sywang@csr.utexas.edu).

Jin Li is with the Shanghai Astronomical Observatory, Chinese Academy of Sciences, Shanghai 100045, China (e-mail: lijin@shao.ac.cn).

Yufeng Nie is with the Department of Land Surveying and Geo-Informatics, The Hong Kong Polytechnic University, Hong Kong SAR, China (e-mail: yufeng.nie@polyu.edu.hk).

Digital Object Identifier 10.1109/JSTARS.2024.3448488

I. Introduction

SATELLITE gravimetry can be regarded as a distinctive remote sensing technique for Earth observation. The gravity recovery and climate experiment (GRACE) and GRACE follow-on (GRACE-FO) satellite missions have provided a revolutionary tool for measuring Earth's gravity field and change over time from space [1]. Since GRACE was launched in 2002 (and GRACE-FO in 2018), GRACE/GRACE-FO measurements have been used to study large-scale water mass variations [1], [2], including changes in terrestrial water storage (TWS) [3], [4], [5], groundwater reservoirs [6], polar ice sheets and mountain glaciers [7], [8], [9], and the global ocean [10], all resulting in a greatly improved understanding of the global water cycle [11]. The data have also provided unique measures of solid Earth deformation due both to glacial isostatic adjustment (GIA) and major earthquakes [12], [13]. Despite such successful applications, the coarse spatial resolution of the GRACE measurement (a few hundred km) makes it challenging to directly validate and assess errors in GRACE gravity spherical harmonic (SH, also called GSM) solutions, and in mass concentration [mascon (MC)] solutions. Earlier studies [14] and [15] showed that water level variations in the Caspian Sea provide a useful signal for validation and error assessment due to the large extent of the Sea and its well-measured water level variations via satellite altimetry. This study makes use of the Caspian Sea signal to evaluate improved and much longer spans of GRACE/GRACE-FO data, which are now available.

GRACE/GRACE-FO missions track intersatellite range and range-rate between two coplanar, low-altitude satellites via a K-band ranging (KBR) system. Each satellite is equipped with a SuperSTAR Accelerometer (ACC), GPS receiver, star cameras, and laser retro reflectors. GRACE-FO satellites are also equipped with a Laser Ranging Interferometer as a test for future missions [16]. The GRACE/GRACE-FO science data system uses the range and range rate and ancillary data to estimate a new gravity field every month, in the form of corrections to a predefined background gravity model [17]. GRACE/GRACE-FO spatial resolution and accuracy depend on satellite orbital configuration (altitude, inclination, intersatellite distance), as

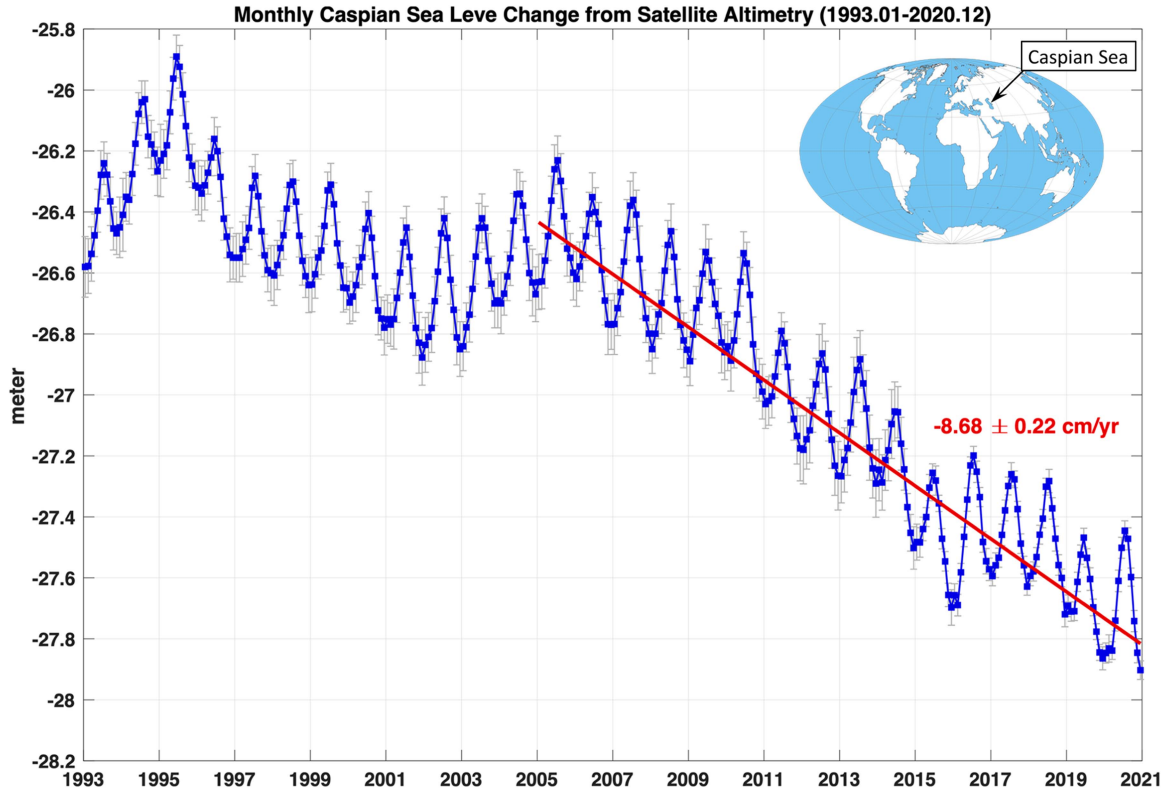

Fig. 1. Monthly CSL change in meters from satellite altimetry (https://hydroweb.theia-land.fr/) over the period January 1993–December 2020. The red line shows the least square fit linear trend (−8.68 ± 0.22 cm/yr) for the period since 2005. Mean CSL is currently about 28 m below the global mean sea level.

well as measurement and processing elements including accuracy of KBR ranging and ACC measurements; quality of geophysical dealiasing models (ocean tides, solid Earth tides, atmospheric tides, atmospheric and oceanic general circulation); and data editing, processing, and calibration procedures. Refinement of measuring and processing elements has led to continued increases in solution quality with each new release (RL) version, currently RL06, which is considerably improved relative to RL05 [18] as used by [15]. However, high-degree and order gravity SH coefficients in GSM solutions continue to be dominated by noise, and relatively large errors are found in some low-degree coefficients. Noise in high degree and order coefficients is usually addressed by spatial smoothing, which exacerbates spatial leakage limitations associated with the finite range of SH coefficients in GSM solutions (degree and order 60 or 96 for RL06) [19].

Validation of GRACE/GRACE-FO satellite gravity observations is challenging because there are few independent observations having comparable spatial and temporal sampling. However, variations in Caspian Sea level (CSL) were shown to provide a useful signal for this purpose (e.g., [14], [15], [20], [21]). CSL change is thought to be dominated by water mass change, with minor contributions from steric effects [20]. As the largest enclosed inland water body with an area near 371 000 km^2 (excluding the Kara–Bogaz–Gol (KBG) lagoon), the Caspian Sea is spatially well-resolved by GRACE/GRACE-FO. Furthermore, the CSL signal is of substantial magnitude, with meter-scale fluctuations in the two decades since the launch of GRACE. Fig. 1 shows satellite altimetry observations with peak-to-peak seasonal oscillations of up to ∼40 cm, and, since 2005, a steady decline near 8.68 cm/year.

Previous studies [22], [23] showed that at the global scale (or in the longest wavelength), there appeared a "systematic" bias between GRACE-FO and satellite altimeter (minus steric effect) estimated global mean ocean mass changes, which was believed to be attributed to the uncertainties of GRACE-FO gravity coefficients of lowest degrees and orders, steric effect estimates, and minor altimeter instrument drift. It is also important to assess the relative accuracies of GRACE and GRACE-FO missions and identify any potential biases between the two missions at regional scales using available independent estimates, such as CSL change.

In this study, we carry out a comprehensive analysis of CSL change using satellite altimetry and the GRACE/GRACE-FO gravity measurements over the period April 2002 to December 2020. The main goals are following:

1) to compare and validate GRACE/GRACE-FO RL06 GSM and MC solutions at regional scales;
2) to evaluate effects of different post-processing [spatial smoothing and/or filtering and leakage correction (LC)] methods on GRACE/GRACE-FO estimates of CSL change;
3) to compare GRACE and GRACE-FO measurements with the CSL altimetry series of Fig. 1 and to identify the presence of any systematic bias between GRACE and GRACE-FO.

II. Datasets and Processing Methods

A. CSL Altimetry Series

The altimetry time series in Fig. 1 is derived from multiple missions (TOPEX/Poseidon, Jason-1, -2 and -3, Geosat Follow-On, Envisat, and others) by the Hydroweb project.[1] This time series represents the mean water level change of the entire Caspian Sea. The original series is irregularly sampledand has been resampled to monthly means. Although calibration of lake level changes from satellite altimetry is somewhat more challenging than for global sea level [24], [43], Hydroweb has been providing time series of altimetry lake level changes in near real time via an automated algorithm. Data for several hundred large lakes and rivers are available, including separate series for the Caspian Sea and KBG. KBG is connected to the Caspian Sea via a narrow channel, but cannot be easily distinguished from the Caspian Sea given the spatial resolution of GRACE/GRACE-FO. Consequently, the CSL altimetry series used here includes the KBG as $\Delta h_{(\mathrm{casp/kbg})}$ via an area weighted average

$$\Delta h_{\mathrm{casp/kbg}} = (\Delta h_{\mathrm{casp}} \times A_{\mathrm{casp}} + \Delta h_{\mathrm{kbg}} \times A_{\mathrm{kbg}}) \,/\, (A_{\mathrm{casp}} + A_{\mathrm{kbg}}) \tag{1}$$

in which Δh_{casp} and Δh_{kbg} are separate water level changes for the Caspian Sea and KBG, and A_{casp} and A_{kbg} are their associated areas. The result is only slightly different from Δh_{casp} because A_{kbg} is only about 5.7% as large as A_{casp}. Given the large area of the Caspian Sea, mean CSL change can also be derived from the average of satellite altimeter sea level anomaly (SLA) grids over the Caspian Sea.

B. GRACE/GRACE-FO GSM Solutions

Separate RL06 GSM solutions are calculated by the three GRACE/GRACE-FO Science Data System centers, the Center for Space Research (CSR) at the University of Texas at Austin, NASA's Jet Propulsion Laboratory (JPL) at the California Institute of Technology, and the German Research Centre for Geosciences (GFZ). All three solutions use a common reference gravity field, the same background geophysical models, and similar data processing methods, although there are some differences among processing and editing strategies. The three solutions used here consist of 4π-fully normalized gravity SH coefficients up to degree and order 60, from April 2002 through December 2020. This period includes 192 monthly solutions, 163 from GRACE (April 2002 to June 2017) and 29 from GRACE-FO (June 2018 to December 2020). All solutions include common gaps of up to a few months during the GRACE era, due to data quality or instrument issues, and about a 1-year gap from the end of the GRACE era until the beginning of GRACE-FO.

We replace certain poorly determined low-degree zonal SH coefficients with independent satellite laser ranging (SLR) solutions. For both GRACE and GRACE-FO, this is done for degree 2 (ΔC_{20}), and ΔC_{30} is also replaced for GRACE-FO. Further discussion is found in the GRACE/GRACE-FO Technical Note 14 [25]. Degree-1 SH coefficients, representing geocenter motion, are absent in GSM solutions, but estimated coefficients (ΔC_{11} ΔS_{11} ΔC_{10}) are determined as described in Technical Note 13 [26]. GSM solutions contain signals associated with solid Earth geophysical processes, including GIA and seismic events. Because the focus here is comparison with CSL, we remove GIA effects using the ICE6G-D model [27]. GSM solutions already have had atmospheric and oceanic signals removed in the dealiasing process [17].

We use two smoothing methods to suppress noise. The first is 300-km Gaussian smoothing and the second is 300-km smoothing plus a decorrelation (DC) filter to remove longitudinal stripes (300 km + DC). DC filtering is omitted in the first case because of its possible effect on CSL signals in GRACE/GRACE-FO data due to the dominantly longitudinal orientation of the Caspian Sea [28]. In the second case, we use a specially designed DC filter. For each SH order (14 and above), we fit by least-squares and remove a polynomial of order 4 to even and odd coefficient pairs (called P4M14). By starting at SH order 14, instead of 6 or 10 as in other studies (e.g., [29], [30]) the effect on a signal the size of the Caspian Sea should be reduced.

After these preprocessing steps, we computed a global $0.5^\circ \times 0.5^\circ$ mass change grid in units of equivalent water height (EWH) from each of the three GSM solutions as ([31])

$$\Delta\sigma\ (\theta,\lambda) = \frac{M}{4\pi a^2 \rho} \sum_{l=1}^{60} \sum_{m=0}^{l} \frac{2l+1}{1+k_l} W_l P_{lm}\,(\cos\theta) \\ (\Delta C_{lm} \cos m\lambda + \Delta S_{lm} \sin m\lambda) \tag{2}$$

in which M is Earth's mass, a its mean radius, ρ water density (1000 kg/m^3), P_{lm} the 4π-normalized associated Legendre functions, C_{lm} and S_{lm} SH (Stokes) coefficients of degree l and order m. W_l is the 300 km Gaussian smoothing weights computed using (32-34) of [31]. GRACE/GRACE-FO estimates of CSL change (cm of EWH) are then computed using a $0.5^\circ \times 0.5^\circ$ basin mask for the combined Caspian Sea and KBG (see Fig. 2), with the cosine of latitude weights. The total area of the basin mask is ~390 000 km^2, very close to the Caspian Sea and KBG combined areas of about 389 000 km^2.[2,3]

Time series of CSR, JPL, and GFZ RL06 GSM estimates of CSL (300-km smoothing, averaged over the mask of Fig. 2) are shown in the top panel of Fig. 3, along with the CSL altimetry series from Fig. 1, all reduced to zero-mean. While all three GRACE/GRACE-FO estimates agree well with one another, they show considerably reduced variation relative to the altimetry series. This is due to spatial leakage of Caspian Sea signals into adjacent arid regions, in part a result of the applied smoothing. Reduced amplitudes are evident both for seasonal and trend components. Amplitudes and phases of least square fit annual and semiannual sinusoids in Table I show amplitudes roughly 50% smaller than the altimetry series. We have omitted (300 km + DC filter) series in Fig. 3, but Table I shows associated seasonal and trend components roughly 1/3 as large as those of the CSL altimetry series, confirming the attenuating effect of DC filtering. DC filtering also affects the phase of the annual components.

[1] [Online]. Avaiable: https://hydroweb.theia-land.fr/.

[2] Online. Available: https://en.wikipedia.org/wiki/Caspian_Sea

[3] Online. Available: https://en.wikipedia.org/wiki/Garabogazk%C3%B6l

TABLE I
LEAST SQUARE ANNUAL AND SEMIANNUAL AMPLITUDES AND PHASES AND TRENDS OF THE CSL ALTIMETRY SERIES AND VARIOUS GRACE/GRACE-FO ESTIMATES FOR APRIL 2002–DECEMBER 2020

CSL Change	Annual		Semiannual		Linear Trend (cm/yr)
	Amplitude (cm)	Phase (deg)	Amplitude (cm)	Phase (deg)	
Altimeter (Caspian Sea)	18.07 ± 1.28	266 ± 4	3.71 ± 1.28	85 ± 20	−7.42 ± 0.17
Altimeter (Caspian Sea/KBG)	17.75 ± 1.28	268 ± 4	3.63 ± 1.28	84 ± 20	−7.55 ± 0.17
CSR GSM (300km, No LC)	6.55 ± 0.53	306 ± 5	1.53 ± 0.53	101 ± 20	−3.16 ± 0.07
JPL GSM (300km, No LC)	6.39 ± 0.54	306 ± 5	1.29 ± 0.55	93 ± 24	−3.22 ± 0.07
GFZ GSM (300km, No LC)	6.52 ± 0.56	309 ± 5	1.94 ± 0.56	85 ± 17	−3.12 ± 0.07
CSR GSM (300km+DC, No LC)	6.06 ± 0.45	312 ± 4	1.38 ± 0.45	98 ± 19	−2.71 ± 0.06
JPL GSM (300km+DC, No LC)	5.91 ± 0.45	314 ± 4	1.34 ± 0.45	91 ± 19	−2.73 ± 0.06
GFZ GSM (300km+DC, No LC)	6.07 ± 0.46	314 ± 4	1.31 ± 0.46	88 ± 20	−2.60 ± 0.06
CSR GSM (300km/SF LC)	17.99 ± 1.44	306 ± 5	4.21 ± 1.44	101 ± 20	−8.66 ± 0.19
JPL GSM (300km/SF LC)	17.53 ± 1.49	306 ± 5	3.53 ± 1.50	93 ± 24	−8.83 ± 0.20
GFZ GSM (300km/SF LC)	17.91 ± 1.54	309 ± 5	5.33 ± 1.55	85 ± 17	−8.56 ± 0.20
CSR GSM (300km+DC/SF LC)	16.63 ± 1.24	312 ± 4	3.78 ± 1.25	98 ± 19	−7.43 ± 0.16
JPL GSM (300km+DC/SF LC)	16.24 ± 1.23	314 ± 4	3.69 ± 1.23	91 ± 19	−7.49 ± 0.16
GFZ GSM (300km+DC/SF LC)	16.66 ± 1.25	314 ± 4	3.60 ± 1.26	88 ± 20	−7.15 ± 0.16
CSR MC (No LC)	8.86 ± 0.97	291 ± 6	2.53 ± 0.97	88 ± 22	−4.76 ± 0.13
CSR MC (150km BF LC)	16.83 ± 1.48	308 ± 5	4.72 ± 1.48	92 ± 18	−8.13 ± 0.19
JPL MC (No LC)	9.39 ± 0.90	295 ± 5	2.48 ± 0.90	73 ± 21	−4.99 ± 0.12
JPL MC (3x3 BF LC)	18.14 ± 1.53	306 ± 5	3.94 ± 1.53	73 ± 22	−9.13 ± 0.20
GSFC MC (no LC)	10.07 ± 1.04	288 ± 6	3.49 ± 1.04	91 ± 17	−7.89 ± 0.14

Note: GRACE/GRACE-FO GSM estimates include three with 300-km Gaussian smoothing, and three with the addition of DC filtering, for the cases of no LC and with SF LC. In addition, amplitudes, phases, and trends for MC estimates are also given. The two CSR MC estimates are without or with 150-km buffer (BF) LCs, and the two JPL MC estimates are without or with 3°x3° BF LC.

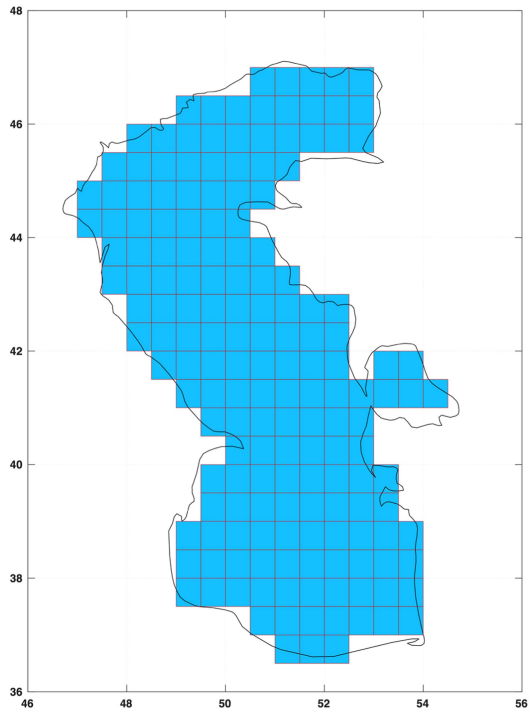

Fig. 2. A 0.5° × 0.5° basin mask for the Caspian Sea and KBG lagoon.

C. Scale Factor LC

The scale factor (SF) method for correcting spatial leakage is easily implemented via a calculation using synthetic data. The synthetic data might be the observed CSL altimetry series, or just a constant assigned to each element of the Caspian Sea mask (see Fig. 1). Then all (0.5° × 0.5°) grid values outside the Caspian Sea mask are set to zero, SH coefficients for the global grid are computed to degree and order 60, 300 km Gaussian smoothing is applied, and (2) is used to compute values over the Caspian Sea mask, which are then added together as described earlier. The SF value is the ratio of true (synthetic) CSL to that computed in the simulated GRACE processing steps and summation over the mask. For this case, the estimated SF only depends on the width of Gaussian filtering and spatial characteristics of the Caspian Sea. The SF is then the multiplied to adjust GRACE/GRACE-FO estimates for spatial leakage and can be determined also for the case where DC filtering is used. For the case of 300-km Gaussian smoothing, the SF value is about 2.745.

The SF method should be effective in this case because the region surrounding the Caspian Sea is quite arid. Although it is also possible to add independent information about (nonzero) values in the surrounding region, for example, from a climate model (discussed below), the simple assumption of zero values leads to much-improved agreement with the altimetry series in Fig. 3(b). Estimates with 300-km smoothing (denoted 300km/SF) are now reasonably similar to the CSL altimetry series in terms of both seasonal and trend components as shown in Table I. However, there are some differences that require further analysis. For example, after SF correction, trends for GSM estimates (with 300-km smoothing) tend to be larger than those of the altimetry series. The addition of DC filtering reduces them somewhat. Annual phases also differ when DC filtering is added. These differences are thought to be related to TWS signals from surrounding regions as discussed in the Section II-D, and possibly to steric changes in CSL, also discussed in a later section [28].

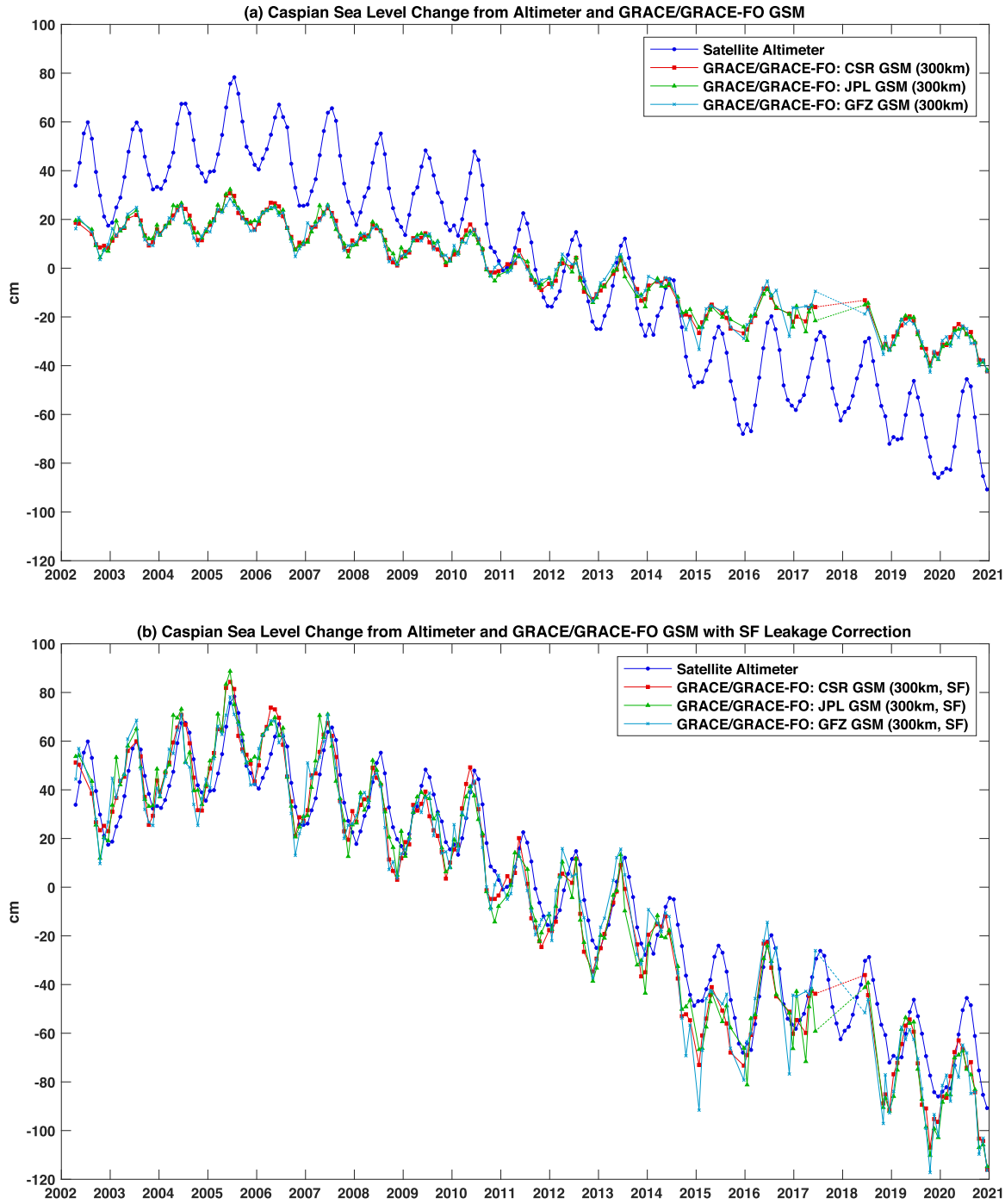

Fig. 3. (a) Monthly CSL change from altimetry (see Fig. 1) and GRACE/GRACE-FO GSM solutions (without LC) for April 2002–December 2020 from CSR, JPL, and GFZ RL06 GSM (300-km Gaussian smoothing). Gaps between GRACE and GRACE-FO series are connected by dashed lines (b) as in (a), but with SF LCs applied as described in the text.

Seasonal amplitudes and phases and trends for the GRACE/GRACE-FO GSM CSL estimates after SF LCs are estimated via unweighted least-squares fit and listed in Table I for comparisons. For consistency, the listed altimeter least-squares fits are estimated after the altimeter CSL series is first resampled at GRACE/GRACE-FO time epochs (or which GRACE/GRACE-FO solutions are available). The different samplings will lead to small but notable differences. Consistent with visual examination, after SF LCs, the three GSM CSL estimates with 300-km smoothing show notably larger decreasing trends (ranging from -8.56 ± 0.20 to -8.83 ± 0.20 cm/yr) than altimeter observations (-7.55 ± 0.17 cm/yr). For the three GSM CSL estimates with 300 km + DC smoothing, the decreasing trends are slightly smaller (7.15 ± 0.16 to -7.49 ± 0.16 cm/yr). At seasonal scales, the most obvious discrepancies are annual phase lags of $\sim$40 degrees for the 300-km smoothing results

TABLE II
ANNUAL AND SEMIANNUAL AMPLITUDES AND PHASES AND TRENDS OF CSL CHANGES FROM SATELLITE ALTIMETRY AND VARIOUS GRACE/GRACE-FO ESTIMATES FOR THE PERIOD APRIL 2002–DECEMBER 2020

CSL Change	Annual		Semiannual		Linear Trend (cm/yr)
	Amplitude (cm)	Phase (deg)	Amplitude (cm)	Phase (deg)	
Altimeter (Caspian Sea/KBG)	17.75 ± 1.28	268 ± 4	3.63 ± 1.28	84 ± 20	−7.55 ± 0.17
CSR GSM (300km, SF, TWS)	18.01 ± 1.49	273 ± 5	4.67 ± 1.50	96 ± 18	−8.35 ± 0.20
JPL GSM (300km, SF, TWS)	17.64 ± 1.56	272 ± 5	4.04 ± 1.56	88 ± 22	−8.52 ± 0.20
GFZ GSM (300km, SF, TWS)	17.30 ± 1.60	276 ± 5	5.91 ± 1.61	82 ± 16	−8.24 ± 0.21
CSR GSM (300km+DC, SF, TWS)	15.29 ± 1.25	276 ± 5	4.11 ± 1.25	93 ± 17	−6.89 ± 0.16
JPL GSM (300km+DC, SF, TWS)	14.78 ± 1.24	276 ± 5	4.06 ± 1.24	86 ± 17	−6.94 ± 0.16
GFZ GSM (300km+DC, SF, TWS)	15.08 ± 1.26	278 ± 5	3.99 ± 1.26	84 ± 18	−6.60 ± 0.17
CSR GSM (300km/300km+DC, SF, TWS)	16.40 ± 1.34	275 ± 5	4.32 ± 1.34	95 ± 18	−7.50 ± 0.18
JPL GSM (300km/300km+DC, SF, TWS)	15.96 ± 1.35	274 ± 5	3.97 ± 1.36	87 ± 19	−7.61 ± 0.18
GFZ GSM (300km/300km+DC, SF, TWS)	15.96 ± 1.37	277 ± 5	4.85 ± 1.38	83 ± 16	−7.30 ± 0.18
CSR MC (150km BF, TWS)	15.56 ± 1.49	287 ± 5	4.73 ± 1.50	89 ± 18	−7.70 ± 0.20
JPL MC (3x3 BF, TWS)	17.32 ± 1.55	279 ± 5	4.15 ± 1.56	69 ± 21	−8.66 ± 0.20
GSFC MC (no LC)	10.07 ± 1.04	288 ± 6	3.49 ± 1.04	91 ± 17	−7.89 ± 0.14

Note: GRACE/GRACE-FO estimates include six CSR, JPL, and GFZ GSM with 300-km Gaussian smoothing (with and without DC filtering) using the revised SF LC that considers TWS, labeled by (300 km, SF, TWS) and (300 km+DC, SF, TWS). Results for the averages of 300 km and 300 km+DC filterings are also shown for each of the three GSM (SF, TWS) solutions, labeled by (300 km/300km+DC, SF, TWS). In addition, results for MC estimates are given for CSR MC with 150-km BF leakage and TWS corrections, JPL MC with 3x3 degree element leakage (3x3 BF) and TWS corrections, and the GSFC MC as discussed in the text.

(and ∼45 degrees for 300 km + DC), which are believed to be related to TWS contributions and steric effects [28]. Further analysis appears in the next section.

GRACE/GRACE-FO CSL estimates can be also derived using the forward modeling (FM) method as used in our previous study [15]. Our additional analysis (not shown here) indicates that the FM results are mostly consistent with the SF estimates after the needed corrections. In the present analysis, we focus on the more straightforward and easy-implemented SF method and demonstrate how we can minimize the striping noise effect on GRACE/GRACE-FO estimates (discussed later).

D. TWS Contributions to GSM Estimates

The preceding SF LC neglected TWS in surrounding regions by assigning zero values in the synthetic data. Although the surrounding region is arid, TWS changes near the Caspian Sea may still contribute to CSL estimates from GSM solutions. We use the global land data assimilation system (GLDAS) NOAH (v2.1) land surface model to predict TWS in surrounding regions, from soil moisture to 2-m depth, snow water, and canopy water [32].

Monthly samples of GLDAS TWS data on a 1° × 1° grid were resampled to the epochs of GRACE/GRACE-FO GSM data. Then TWS change grids were converted to SH, truncated at degree and order 60, Gaussian smoothed with a 300-km filter, and resampled on a 0.5° × 0.5° grid. The result is subtracted from GRACE/GRACE-FO GSM estimates (both 300 km or 300 km + DC filtering), and then SF LC is determined as described above.

Fig. 4(a) shows CSR RL06 GSM CSL change estimates (both 300 km and 300 km + DC filtering) using this revised SF LC, along with the CSL altimetry series. Fig. 4(a) omits JPL and GFZ GSM estimates for clarity and shows that agreement between the CSR GSM estimate and the CSL altimetry series is much improved relative to Fig. 3(b). Table II quantifies this improvement relative to Table I, showing seasonal amplitudes and phases and trends for the 6 RL06 GSM CSL estimates (3 for 300 km and 3 for 300 km + DC filtering). For example, using the revised SF correction (with TWS), annual phase differences drop from the range of 40°–45° to about 5°–10°. Table II shows also that DC filtering has attenuated RL06 GSM seasonal and trend signals.

The DC filter is not a linear filter, making it difficult to quantify its effect on estimates from GSM data. Omitting it likely leaves longitudinal stripe noise contaminating CSL estimates, especially their trends. Including DC filtering is likely to attenuate amplitudes given the north–south orientation of the Caspian Sea. This suggests that an average of the two (denoted by 300 km/300 km + DC in Table II and Fig. 4) may provide an improved estimate. Fig. 4(b) with seasonal components removed indicates that this average does improve agreement with the altimetry series at periods longer than one year. Table II shows that the average has improved seasonal and trend agreement for all three processing center solutions.

E. GRACE/GRACE-FO MC Solutions

There are three available GRACE/GRACE-FO RL06 mass concentration (mascon) solutions from CSR, JPL, and the NASA Goddard Space Flight Center (GSFC) for the same April 2002 to December 2020 period of GSM solutions. These are presented as mass change grids and are termed as level-3 data. Common postprocessing steps for computing the three MC solutions include replacing ΔC_{20} and ΔC_{30} with SLR solutions, inclusion of estimated degree-1 coefficients, and removal of GIA effects as described earlier for GSM solutions. Over the ocean, atmospheric and oceanic effects are restored to give ocean bottom pressure (OBP) estimates.

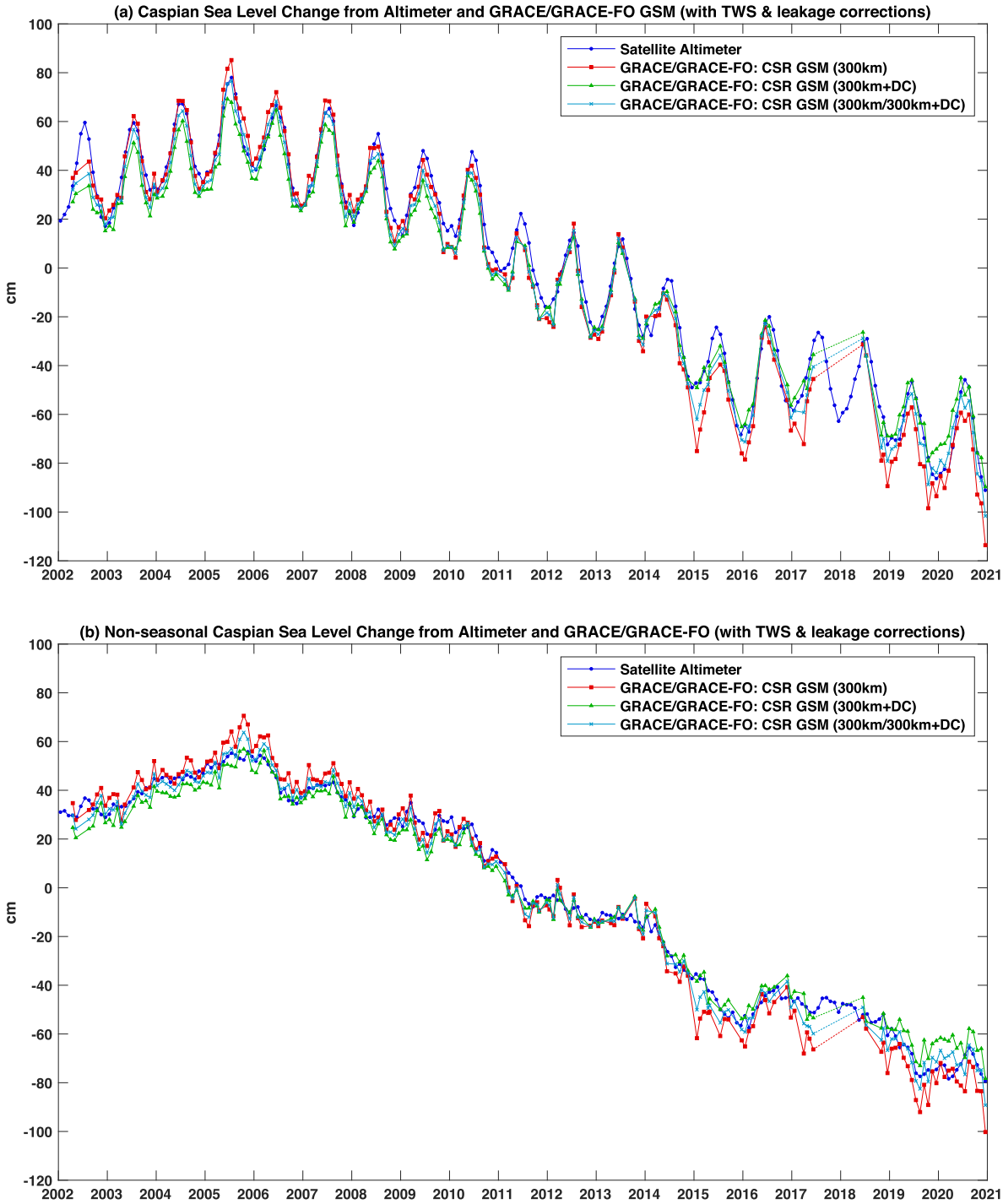

Fig. 4. (a) Monthly CSL from satellite altimetry and CSR GSM estimates corrected using the revised SF method that includes TWS effects (from GLDAS Noah V2.1). GSM estimates include 300-km Gaussian filtering with and without DC filtering, and the average of the two (300 km/300 km + DC). Gaps between GRACE and GRACE-FO series are connected by dashed lines. (b) Is similar to (a), but with annual and semiannual variations removed from all series. Table II gives amplitudes and phases of seasonal terms that have been removed.

In general, MC s offer improved spatial resolution and reduced longitudinal striping noise relative to GSM solutions. However, there are differences among the three MC solutions in terms of the grid spacing that defines their nominal spatial resolution. For example, CSR Version-2 MC s are computed for $1^\circ \times 1^\circ$ equal-area elements using a regularization method [33] and then represented on a $0.25^\circ \times 0.25^\circ$ grid, allowing for improved coastline grid separation [34]. However, actual spatial resolution is probably poorer than $1^\circ \times 1^\circ$, considering fundamental limitations imposed by the GRACE/GRACE-FO orbital configuration and measurement system, and by the 200-km Gaussian smoothing applied in the processing [33].

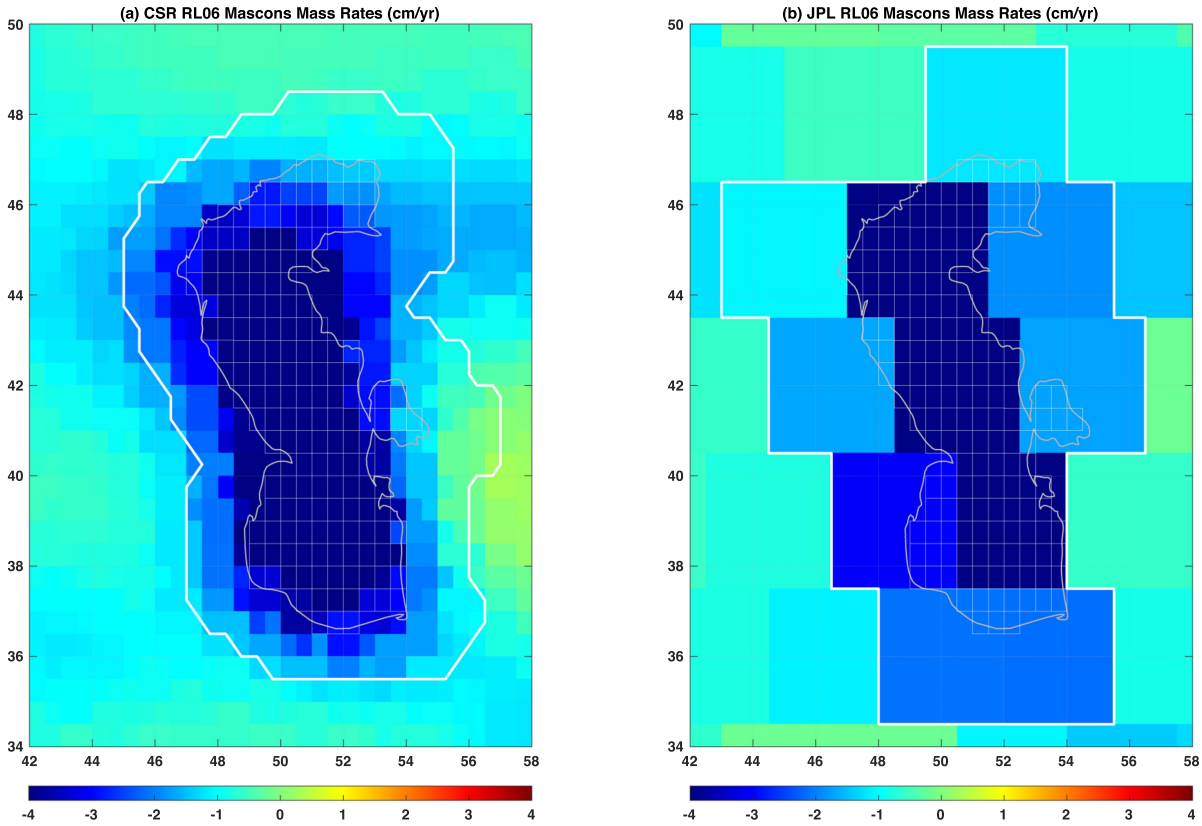

Fig. 5. BF zones used for correcting leakage for (a) CSR and (b) JPL RL06 MC CSL change estimates. The CSR BF zone includes grid values within 150 km of the coast area, circled by the thick white lines in (a). The JPL BF zone includes all 3° × 3° MC elements that overlap the Caspian Sea, circled by the thick white lines in (b).

JPLVersion-2 MC s are determined for 3° × 3° equal-area elements directly from GRACE/GRACE-FO level-1 data and resampled on 0.5° × 0.5° grids [35], [36]. A separate version is also available that employs a Coastline Resolution Improvement (CRI) filter to reduce leakage between land and oceans, although the CRI filter is not applied to the Caspian Sea and other lakes. Additionally, JPL solutions come with SFs to correct for spatial leakage within each 3° × 3° equal-area element derived using the community land model.

GSFC V1.0 MC s are initially calculated for 1° × 1° equal-area elements (area ∼12390 km^2) from Level-1B data (KBRR, GPS orbits, ACC, and other data). These are combined into large geographical regions, for example, Antarctica, Greenland, land, oceans, the Caspian Sea, and others, which should reduce spatial leakage problems [37]. Thus GSFC MC estimates of CSL do not require further correction for spatial leakage. The GSFC RL06 MC solutions include two separate versions with different definitions for ocean MCs, representing either OBP or SLA. The SLA version is used in the present analysis. We can simply add all Caspian Sea MCs to get the total or mean CSL changes (by dividing the total volume change by the area of Caspian Sea). Our JPL MC estimate of CSL is computed using the 0.5° × 0.5° Caspian Sea mask with cosine latitude weights, as described above for GSM estimates. CSR MC estimates are obtained by resampling 0.25° × 0.25° values onto 0.5° × 0.5° grids, before summing over the Caspian Sea mask.

Although MCs offer nominally improved spatial resolution, they may still suffer from spatial leakage associated with fundamental resolution limits of the GRACE/GRACE-FO measurement. This is most likely for CSR and JPL solutions (see Fig. 5). Following the earlier study of [28], leakage of Caspian Sea signals into surrounding areas can be addressed approximately by including signals from BF zones around the Caspian Sea. The choice of BF zone size is somewhat arbitrary, so differing choices may lead to different estimates. Our choice of BF zone sizes improves agreement with altimetry, but the need for this correction shows the challenges of using MC solutions for relatively small water bodies such as the Caspian Sea. Additional LCs for TWS are discussed below.

For CSR MCs, we include signals from a BF zone consisting of all grid points within 150 km of the coast, the area enclosed by thick white lines in Fig. 5(a). The JPL BF zone includes all 3° × 3° MC elements overlapping the Caspian Sea as shown by the thick white lines in Fig. 5(b). The map colors show the least square fit mass rates for the two MC solutions from April 2002 to December 2020.

Table I gives seasonal and trend components for CSR and JPL MCs (with and without BF zone corrections for leakage), showing that omitting BF zone corrections results in greatly reduced variability relative to CSL altimetry. On the other hand, GSFC MC estimates agree very well with CSL altimetry in rate (−7.89 ± 0.14 vs. −7.55 ± 0.17 cm/yr). This suggests that

TABLE III
SEASONAL AND TREND COMPONENTS OF CSL CHANGES FROM SATELLITE ALTIMETRY AND FROM SIX GRACE/GRACE-FO ESTIMATES AFTER WOA13 STERIC CORRECTIONS FOR APRIL 2002–DECEMBER 2020

CSL Change	Annual		Semiannual		Linear Trend (cm/yr)
	Amplitude (cm)	Phase (deg)	Amplitude (cm)	Phase (deg)	
Altimeter (Caspian Sea/KBG)	17.75 ± 1.28	268 ± 4	3.63 ± 1.28	84 ± 20	−7.55 ± 0.17
CSR GSM (300km/300km+DC, TWS, Steric)	18.44 ± 1.34	266 ± 4	4.25 ± 1.34	91 ± 18	−7.50 ± 0.18
JPL GSM (300km/300km+DC, TWS, Steric)	18.02 ± 1.35	266 ± 4	3.95 ± 1.36	83 ± 20	−7.61 ± 0.18
GFZ GSM (300km/300km+DC, TWS, Steric)	17.91 ± 1.37	268 ± 4	4.85 ± 1.38	79 ± 16	−7.30 ± 0.18
CSR MC (150km BF, TWS, Steric)	17.05 ± 1.49	277 ± 5	4.70 ± 1.50	85 ± 18	−7.70 ± 0.20
JPL MC (3x3 BF, TWS, Steric)	19.16 ± 1.55	271 ± 5	4.22 ± 1.56	65 ± 21	−8.66 ± 0.20
GSFC MC (no LC, Steric)	11.62 ± 1.04	273 ± 5	3.45 ± 1.04	86 ± 17	−7.89 ± 0.14

Note: These include three GSM average estimates (300km/300km+DC) with SF leakage and TWS corrections, and three MC estimates including buffer zone (BF) and TWS corrections for CSR and JPL solutions, and none for GSFC MC.

GSFC basin-scale MCs have successfully suppressed spatial leakage of Caspian Sea signals into surrounding regions. However, it is puzzling that the GSFC annual amplitude is much smaller than that of the CSL altimetry series (10.07 ± 1.04 vs. 17.75 ± 1.28 cm). The three MC CSL time series are compared with the altimetry series in Fig. 6.

CSR and JPL MC solutions may also be contaminated by land-to-sea leakage. We again use GLDAS NOAH (V2.1) TWS values to correct this. For CSR solutions, we expand GLDAS fields into SH, truncate to degree and order 60, apply 200-km Gaussian smoothing (consistent with 200-km smoothing in CSR RL06 MC computation), and sample this on a 0.5° × 0.5° grid. These TWS changes are then subtracted from values within the CSL mask including the BF zone [see Fig. 5(a)]. For JPL MCs, TWS leakage is computed from samples of the truncated SH expansion of GLDAS fields without smoothing. The result is subtracted from JPL MCs including the BF zone as in Fig. 5(b). In principle, there is no need to correct GSFC solutions for land-to-sea leakage. Seasonal and trend components for the CSR and JPL MC CSL estimates with BF zone leakage and TWS corrections are given in Table II and show improved agreement with the altimetry series relative to those with only the BF correction.

F. Steric Corrections to GRACE/GRACE-FO CSL Estimates

Proper corrections for steric sea level effects in the CSL time series require Caspian Sea temperature and salinity observations, which are very limited. An alternative might be to examine open ocean steric effects at comparable latitudes using Argo float data [38] but this would provide only qualitative insight [28]. Here we use published seasonal steric CSL changes from [20] which we denote as WOA13. These are based on the World Ocean Atlas (WOA 2013) climatology of gridded temperature and salinity fields for the Caspian Sea [39]. We add these to GRACE/GRACE-FO CSL estimates, rather than subtract them from the CSL altimetry series. WOA13 corrections are small but do improve seasonal component agreement with the CSL altimetry series, further reducing differences in phase. Table III gives seasonal and trend components after SF leakage, GLDAS TWS, and WOA13 steric corrections to GSM average series (300 km/300 km + DC) and the three MC estimates. Fig. 7(a) shows a series with these corrections, namely the average CSR GSM time series (300 km/300 km + DC) and CSR MC, as well as the CSL altimetry. In Fig. 7(b), seasonal variations have been removed.

After leakage, TWS, and steric corrections, both GSM average and MC CSL estimates agree remarkably well with the CSL altimetry series in both seasonal and trend components. The slight overestimation of CSL changes by the JPL MCs is likely related to the 3° × 3° BF zone [see Fig. 5(b)] used in LC. Fig. 8(a) uses an annual phasor diagram to show how various corrections lead to improved agreement with the CSL altimetry series. This is more informative than comparing values in the tables. The annual phasor diagrams of altimeter observations and six GRACE/GRACE-FO CSL estimates (three GSM ensemble mean and three MC estimates as listed in Table III) are shown in Fig. 8(b) for comparison. It is clear from Fig. 8(a) that TWS correction plays an important role in improving GSM CSL change estimates, especially in reducing the annual phase differences. Steric effects are small, but not negligible.

G. RMS and Correlation Analyses

Table IV gives root-mean-square (RMS) measures of difference time series computed between the CSL altimetry series and the six GRACE/GRACE-FO estimates in Table III. RMS values are given for simple difference time series and difference series after removing trends. The lowest RMS value in each case appears in bold font. Whether or not trends are retained, the CSR GSM average series show the smallest RMS value among the six GRACE/GRACE-FO estimates. For the simple differences (column one in Table IV), JPL MC estimates have the largest RMS difference relative to the altimetry series. This is due to its larger trend relative to the others (see Table III). After removing trends there is only a slight reduction in RMS values for the three GSM average series and for the CSR MC estimate. This is due to their excellent trend agreement with the altimetry series. The GSFC MC series shows a relatively large RMS difference relative to altimetry (after detrending) related to its underestimation of annual variations.

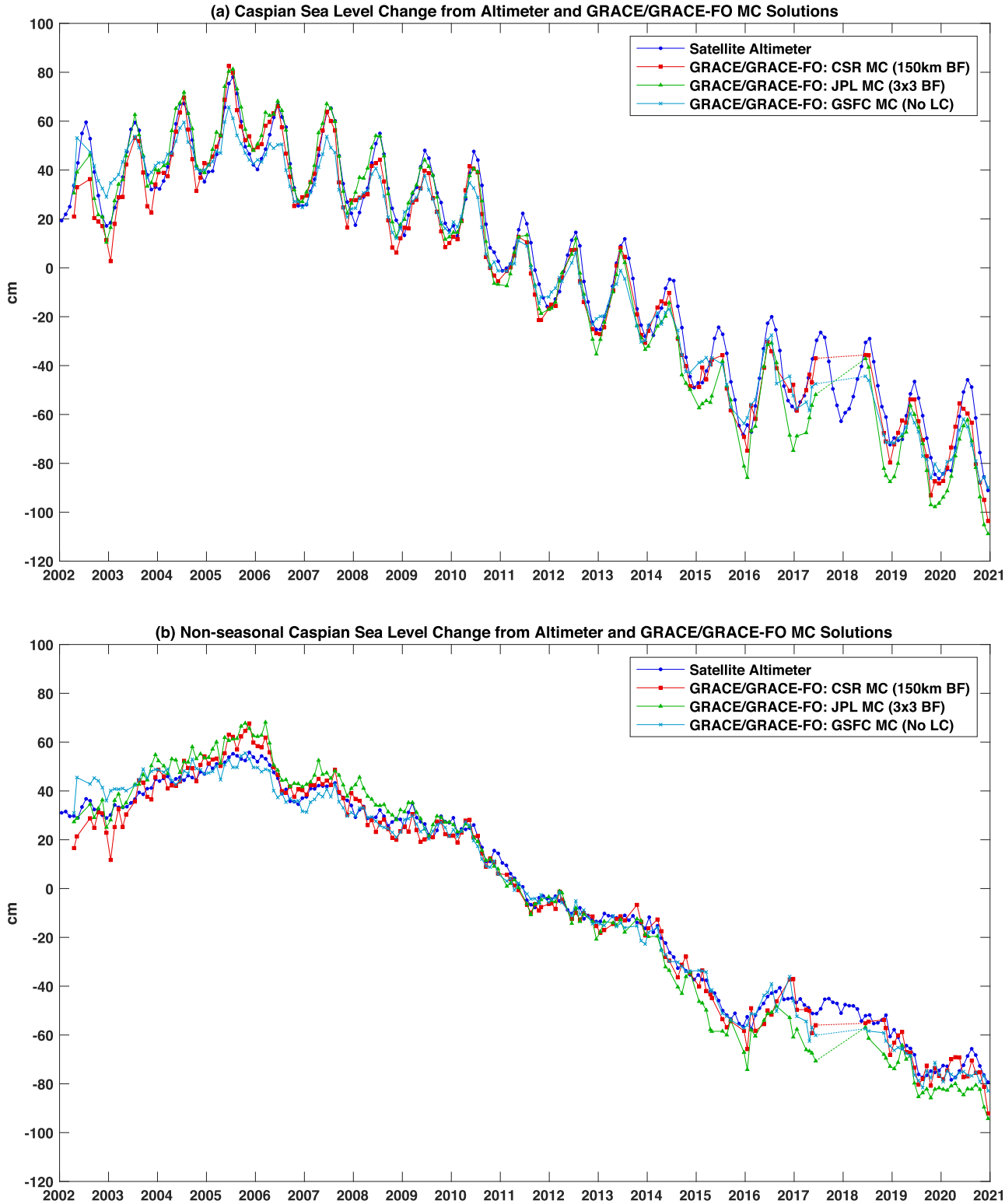

Fig. 6. (a) Monthly CSL from altimetry and the three MC solutions for April 2002–December 2020. The CSR series adds signals from a 150-km BF to reduce leakage. The JPL solutions are corrected for signal leakage by adding signals from all 3×3 degree elements overlapping the Caspian Sea (noted as 3×3 BF). TWS contributions are removed from the BF zones using the GLDAS model as described in the text. The 1-year gaps between GRACE and GRACE-FO are connected by dashed lines (b) similar to (a), but with annual and semiannual variations removed from all-time series.

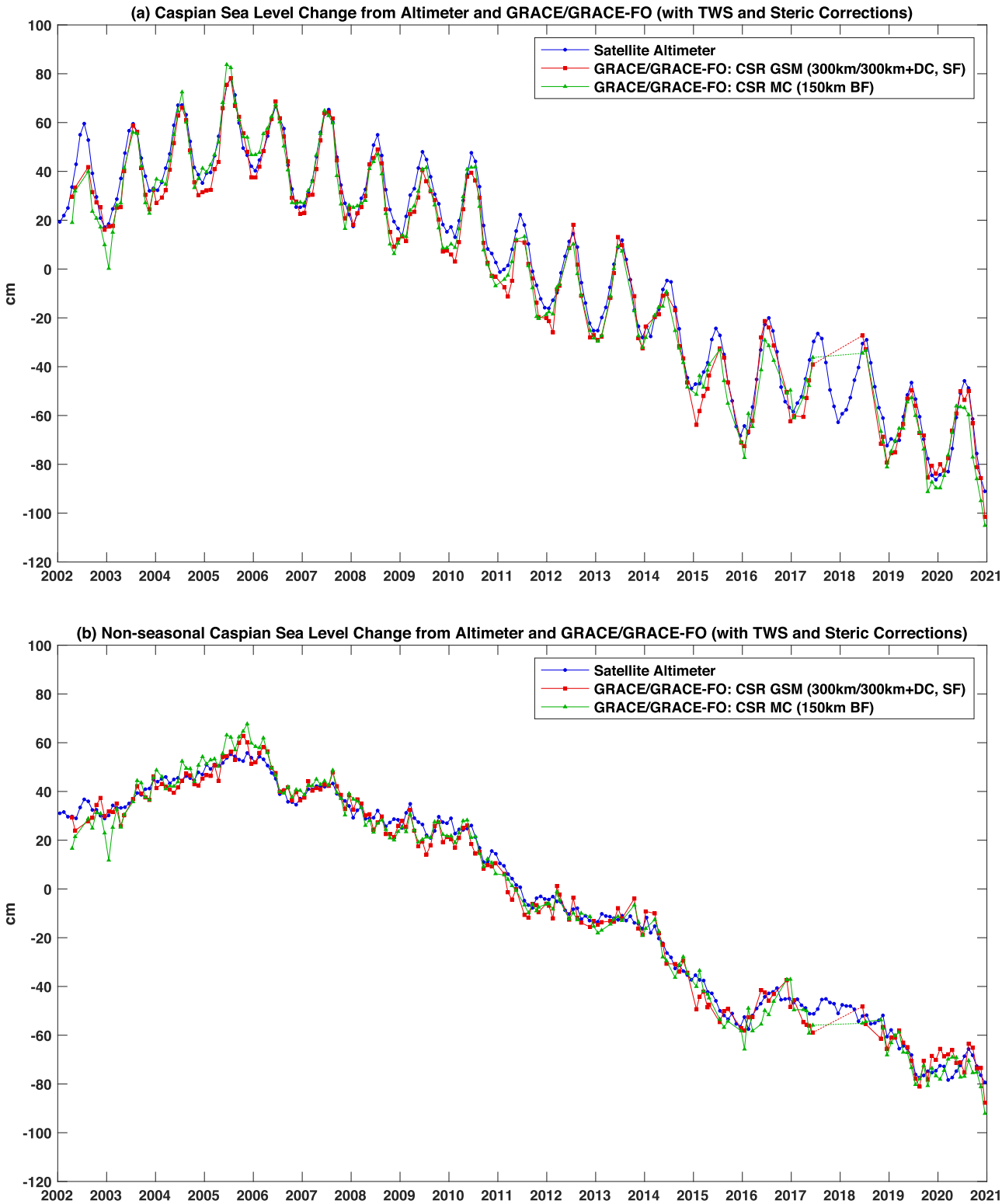

Fig. 7. (a) CSR time series with WOA13 steric and GLDAS TWS corrections for April 2002–December 2020. CSR estimates include CSR GSM with SF LC, and CSR MC with the 150-km BF zone LC. CSR GSM estimates are the average of 300 km and 300 km + DC time series. The gaps between GRACE and GRACE-FO are connected by dashed lines (b) similar to (a), but with annual and semiannual variations removed from all series.

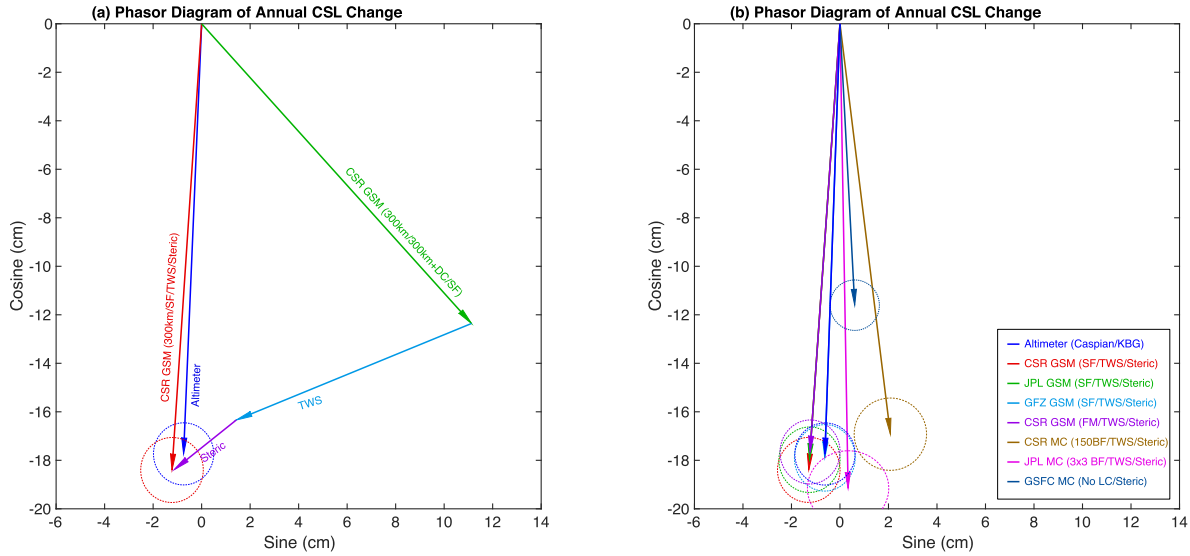

Fig. 8. (a) Phasor diagram of annual CSL changes from the altimetry series, and as derived from GRACE/GRACE-FO CSR GSM (300 km/300 km + DC, SF), with and without TWS and steric corrections. (b) Phasor diagram of annual CSL from altimetry and six different estimates from GRACE/GRACE-FO as listed in Table III. Uncertainties associated with annual amplitudes and phases are shown by the dashed ellipses (in the same color as the vector).

TABLE IV
RMS DIFFERENCES (UNITS OF CM) BETWEEN CSL ALTIMETRY AND VARIOUS GRACE/GRACE-FO ESTIMATES FOR APRIL 2002–DECEMBER 2020

RMS and Corr. Pairs	RMS (Direct Difference)	RMS (Trend Removed)	Correlation (Seasonal/Trend Removed)
Altimeter/CSR GSM (300km/300km+DC, SF)	4.43	4.42	0.94
Altimeter/JPL GSM (300km/300km+DC, SF)	5.14	5.13	0.92
Altimeter/GFZ GSM (300km/300km+DC, SF)	6.10	5.94	0.90
Altimeter/CSR MC (150km BF)	5.34	5.29	0.95
Altimeter/JPL MC (3x3 BF)	7.81	5.01	0.96
Altimeter/GSFC MC (no LC)	6.38	6.11	0.95

Note: The six GRACE/GRACE-FO estimates are the same as in Table III (3 from GSM SF and 3 from MC). RMS differences are given for two cases: 1) simple differences between altimetry and GRACE/GRACE-FO series, and 2) differences after trends are removed. The correlation coefficients between altimetry and GRACE/GRACE-FO series (annual and semiannual and trends removed) appear in the last column.

TABLE V
RMS DIFFERENCES BETWEEN THE CSL ALTIMETRY SERIES AND SIX DIFFERENT GRACE/GRACE-FO ESTIMATES

RMS Pairs (cm)	RMS GRACE/GRACE-FO (2002.04-2020.12)	RMS GRACE (2002.04-2017.06)	RMS GRACE-FO (2018.06-2020.12)
Altimeter/CSR GSM (300km/300km+DC, SF)	4.42	4.28	5.11
Altimeter/JPL GSM (300km/300km+DC, SF)	5.13	5.19	4.79
Altimeter/GFZ GSM (300km/300km+DC, SF)	5.94	5.93	6.03
Altimeter/CSR MC (150km BF)	5.29	5.22	5.68
Altimeter/JPL MC (3x3 BF)	5.01	4.92	5.49
Altimeter/GSFC MC (no LC)	6.11	6.08	6.31

Correlation coefficients between the CSL altimetry series and the six GRACE/GRACE-FO CSL estimates (after seasonal variations and trends are removed) appear in the last column of Table IV. Values range from 0.90 to 0.96, which would be considered significant at the 99% confidence level of 0.20, for an approximate 192 degrees of freedom [40]. The actual degrees of freedom should be smaller than 192 due to the removal of seasonal and trend signals, but this will only slightly increase the confidence level and not affect the conclusion. The JPL MC series shows the highest correlation coefficient.

RMS differences were computed separately for GRACE (April 2002–June 2017) and GRACE-FO (June 2018–December 2020) eras (trends for the entire period were first removed). These should provide a measure of relative accuracies of GRACE and GRACE-FO estimates. The results appear in Table V (columns 3 and 4). RMS differences for the entire period

appear also to facilitate comparison. Most GRACE-era series show smaller RMS differences relative to GRACE-FO. However, the JPL GSM average estimates yield lower RMS values during the GRACE-FO era (4.79 vs. 5.19 cm), distinctly smaller than others in the GRACE-FO era (in the range of 5.11–6.31 cm). Over the GRACE era, CSR GSM average estimates show the smallest RMS (4.28 cm), and the second smallest for JPL MC estimates.

III. Conclusion

CSL changes from satellite altimetry provide a uniquely well-defined signal to evaluate GRACE/GRACE-FO gravity measurements and commonly employed postprocessing and correction methods. The CSL altimetry series is considered the true signal. The study period includes the entire GRACE era and the first few years of GRACE-FO, and the analysis is based on the most recent data release RL06, which is significantly improved relative to earlier releases. Gravity estimates of CSL change are computed from RL06 GSM solutions produced by the three processing centers, CSR, JPL, and GFZ, and from three MC solutions from CSR, JPL, and GSFC.

Two standard filtering schemes for GSM (spherical harmonic) solutions are 300 km Gaussian smoothing, and 300 km smoothing combined with DC filtering to suppress longitudinal stripe noise. An average of these two (300 km and 300 km + DC) was computed with the expectation that it would combine strengths and mitigate weaknesses of each. This was confirmed by improved agreement with the CSL altimetry series, indicating that the average both diminishes stripe noise and limits signal attenuation of the north–south oriented Caspian Sea in DC filtering. For example, trends of the three average GSM series range from -7.30 ± 0.18 to -7.61 ± 0.18 cm/yr, close to the CSL altimetry rate of -7.55 ± 0.17 cm/yr. Annual amplitudes range from 17.91 ± 1.37 to 18.44 ± 1.34 cm, in good agreement with 17.75 ± 1.28 cm from the CSL altimetry series. Compared to GRACE/GRACE-FO GSM estimates, the three MC solutions show relatively larger discrepancies with satellite altimeter observations, especially the GSFC MC solutions.

After fully correcting the six GRACE/GRACE-FO estimates of CSL, we find the CSR RL06 GSM average series is closest to the CSL altimetry series (smallest RMS difference, Table IV), while the JPL RL06 MCs show the highest correlation with altimetry. No obvious biases are found between GRACE and GRACE-FO, but GRACE-FO shows larger RMS differences with altimetry than GRACE. This is consistent with previous GRACE/GRACE-FO error analyses at global scales [18]. The GSFC MCs significantly underestimate annual CSL change, while agreeing well with altimeter observations at interannual and long-term scales (see more discussion later).

IV. Discussion

Spatial leakage associated with GRACE/GRACE-FO estimates is a recognized problem, arising both from the limited range of SH and the filtering noted in the preceding paragraph. Without any LCs, GRACE/GRACE-FO estimates of a relatively isolated signal like the Caspian Sea are reduced in magnitude by about 50%, due to leakage of CSL signal into surrounding arid regions. Even without any spatial smoothing or filtering applied, the attenuation effect due to the 60-degree and -order SH truncation would still reduce the CSL amplitude by about 35%, which is consistent with estimates from a recent analysis [41]. MC estimates from CSR and JPL are also subject to leakage, despite nominally improved resolution associated with small MC elements. We tested a number of approaches to LC. Simple SF correction assuming an isolated Caspian Sea with zero signal in surrounding arid regions leads to significantly improved agreement with the CSL altimetry series for both seasonal and trend components. However, the phase of seasonal signals is in poor agreement.

LC for CSR and JPL MC estimates can be implemented approximately by including signals from a surrounding BF zone. We chose 150 km for CSR and, for the larger JPL $3^\circ \times 3^\circ$ elements, we included all elements that overlap the Caspian Sea. These choices improved agreement with the CSL altimetry series, but seasonal phases are off, as for SF-corrected GSM solutions. Although the choice of BF zone size is somewhat arbitrary, our results suggest that some sort of LC is needed for MC estimates in smaller regions such as the Caspian Sea.

GSFC MC elements are computed for larger regions, including one specifically for the Caspian Sea. It is not clear how one might correct GSFC MCs for leakage, and a good agreement with the CSL altimetry series at long-term time scales [see Fig. 6(b)] suggests a correction is not needed. However, the GSFC MC annual amplitude is substantially smaller than that of the CSL altimetry series. A previous study [20] showed fairly good agreements between the GSFC MC and altimeter CSL estimates at a seasonal scale as well. The altimeter results in [20] were based on the Copernicus Marine Environment Monitoring Service (CMEMS) SLA grids, which appeared to have underestimated seasonal amplitudes of CSL change. A recent study [42] suggested that the large discrepancy between the Hydroweb and CMEMS CSL estimates at seasonal scales was due to the wrong inverted barometer corrections applied in the CMEMS SLA grids over the Caspian Sea. Therefore, further validations of the GSFC MCs are clearly needed.

An additional element of spatial leakage in CSL estimates is associated with TWS changes in surrounding areas. We used the GLDAS model to estimate these. It provides a time series of TWS gridded values from assimilated space and terrestrial observations to include water stored within the upper 2 m and in vegetation and snow. Even though the region surrounding the Caspian Sea is generally arid, correcting for TWS is important, especially for seasonal variations, both for GSM and MC (CSR and JPL) estimates. TWS corrections greatly improve agreement with the CSL altimetry series in annual component phases.

Steric changes alter sea level measured by altimetry, but do not affect mass change measured by GRACE/GRACE-FO, so agreement between CSL altimetry and gravity estimates should improve if a steric correction is applied. There is limited temperature and salinity data available for the Caspian Sea. Seasonal steric change estimates (WOA13, [20]) indicate that

steric effects are relatively small, but that WOA13 corrections do improve agreement between the CSL altimetry series and GRACE/GRACE-FO estimates. No estimate is available of steric contributions to trend or other long-period components of the CSL altimetry series.

ACKNOWLEDGMENT

The authors are grateful to the three anonymous reviewers for their comprehensive and insightful comments, which have led to improved presentation of the results, and would like to thank the GRACE/GRACE-FO Science Data System for providing GSM and mascon solutions (via NASA Earthdata at https://www.earthdata.nasa.gov/), GSFC Geodesy and Geophysics Laboratory for providing GSFC mascon solution (https://earth.gsfc.nasa.gov/geo/data/grace-mascons), and the Hydroweb (https://hydroweb.theia-land.fr/) for providing satellite altimeter data.

REFERENCES

[1] B. D. Tapley et al., "Contributions of GRACE to understanding climate change," *Nature Clim. Change*, vol. 5, no. 5, pp. 358–369, Apr. 2019, doi: 10.1038/s41558-019-0456-2.

[2] J. Chen et al., "Applications and challenges of GRACE and GRACE follow-on satellite gravimetry," *Surv. Geophys.*, vol. 43, no. 1, pp. 305–345, 2022, doi: 10.1007/s10712-021-09685-x.

[3] J. Lu, L. Jia, J. Zhou, M. Jiang, Y. Zhong, and M. Menenti, "Quantification and assessment of global terrestrial water storage deficit caused by drought using GRACE satellite data," *IEEE J. Sel. Topics Appl. Earth Observ. Remote Sens.*, vol. 15, pp. 5001–5012, Jun. 2022, doi: 10.1109/jstars.2022.3180509.

[4] C. Xiao et al., "Monitoring the catastrophic flood with GRACE-FO and near-real-time precipitation data in Northern Henan Province of China in July 2021," *IEEE J. Sel. Topics Appl. Earth Observ. Remote Sens.*, vol. 16, pp. 89–101, Nov. 2022, doi: 10.1109/jstars.2022.3223790.

[5] J. Guo, T. Shi, X. Jin, X. Liu, B. Zhao, and X. Qiao, "Geodetic analysis of orthometric height variations in mainland China using GRACE, hydrological models, and GPS data," *IEEE Trans. Geosci. Remote Sens.*, vol. 62, Apr. 2024, Art. no. 4504815, doi: 10.1109/tgrs.2024.3386879.

[6] N. Iqbal, F. Hossain, H. Lee, and G. Akhter, "Satellite gravimetric estimation of groundwater storage variations over Indus Basin in Pakistan," *IEEE J. Sel. Topics Appl. Earth Observ. Remote Sens.*, vol. 9, no. 8, pp. 3524–3534, Aug. 2016, doi: 10.1109/jstars.2016.2574378.

[7] M. He, Z. Li, W. Jiang, Y. Pan, J. Jiao, and Y. Xiao, "Seasonal and interannual fluctuations of glacier mass balance and climate response processes on the Tibetan Plateau based on GRACE/GRACE-FO," *IEEE Trans. Geosci. Remote Sens.*, vol. 61, Jun. 2023, Art. no. 4301709, doi: 10.1109/tgrs.2023.3280714.

[8] X. Su et al., "High-resolution interannual mass anomalies of the Antarctic ice sheet by combining GRACE gravimetry and ENVISAT altimetry," *IEEE Trans. Geosci. Remote Sens.*, vol. 56, no. 1, pp. 539–546, Jan. 2018, doi: 10.1109/tgrs.2017.2751070.

[9] D. Mu, "Instantaneous rate of ice mass changes in Antarctica observed by satellite gravimetry," *IEEE Geosci. Remote Sens. Lett.*, vol. 15, no. 6, pp. 823–827, Jun. 2018, doi: 10.1109/lgrs.2018.2813362.

[10] B. A. Melzer and B. Subrahmanyam, "Evaluation of GRACE mascon gravity solution in relation to interannual oceanic water mass variations," *IEEE Trans. Geosci. Remote Sens.*, vol. 55, no. 2, pp. 907–914, Feb. 2017, doi: 10.1109/tgrs.2016.2616760.

[11] M. Rodell et al., "Emerging trends in global freshwater availability," *Nature*, vol. 557, no. 7707, pp. 651–659, May 2018, doi: 10.1038/s41586-018-0123-1.

[12] M. E. Tamisiea, J. X. Mitrovica, and J. L. Davis, "GRACE gravity data constrain ancient ice geometries and continental dynamics over Laurentia," *Science*, vol. 316, no. 5826, pp. 881–883, May 2007, doi: 10.1126/science.1137157.

[13] S. C. Han, C. K. Shum, M. Bevis, C. Ji, and C. Y. Kuo, "Crustal dilatation observed by GRACE after the 2004 Sumatra-Andaman earthquake," *Science*, vol. 313, no. 5787, pp. 658–662, Aug. 2006, doi: 10.1126/science.1128661.

[14] S. Swenson and J. Wahr, "Multi-sensor analysis of water storage variations of the Caspian Sea," *Geophys. Res. Lett.*, vol. 34, no. 16, p. L16401, 2007, doi: 10.1029/2007gl030733.

[15] J. L. Chen, C. R. Wilson, B. D. Tapley, H. Save, and J. F. Cretaux, "Long-term and seasonal Caspian Sea level change from satellite gravity and altimeter measurements," *J. Geophys. Res. Solid Earth*, vol. 122, no. 3, pp. 2274–2290, 2017, doi: 10.1002/2016jb013595.

[16] F. W. Landerer et al., "Extending the global mass change data record: GRACE follow-on instrument and science data performance," *Geophys. Res. Lett.*, vol. 47, no. 12, 2020, Art. no. e2020GL088306, doi: 10.1029/2020gl088306.

[17] S. Bettadpur, "CSR level-2 processing standards document for product release 06," Center Space Res., Univ. Texas Austin, Austin, TX, USA, 2018.

[18] J. Chen et al., "Error assessment of GRACE and GRACE follow-on mass change," *J. Geophys. Res. Solid Earth*, vol. 126, no. 9, 2021, Art. no. e2021JB022124, doi: 10.1029/2021jb022124.

[19] Z. Chen, W. Zheng, W. Yin, X. Li, and M. Ma, "Improving spatial resolution of GRACE-derived water storage changes based on geographically weighted regression downscaled model," *IEEE J. Sel. Topics Appl. Earth Observ. Remote Sens.*, vol. 16, pp. 4261–4275, May 2023, doi: 10.1109/jstars.2023.3272916.

[20] B. D. Loomis and S. B. Luthcke, "Mass evolution of Mediterranean, Black, Red, and Caspian Seas from GRACE and altimetry: Accuracy assessment and solution calibration," *J. Geodesy*, vol. 91, no. 2, pp. 195–206, 2016, doi: 10.1007/s00190-016-0952-3.

[21] H. H. Farahani et al., "A high resolution model of linear trend in mass variations from DMT-2: Added value of accounting for coloured noise in GRACE data," *J. Geodynamics*, vol. 103, pp. 12–25, 2017, doi: 10.1016/j.jog.2016.10.005.

[22] J. Chen et al., "Global ocean mass change from GRACE and GRACE follow-on and altimeter and argo measurements," *Geophys. Res. Lett.*, vol. 47, no. 22, 2020, Art. no. e2020GL090656, doi: 10.1029/2020gl090656.

[23] A. Barnoud et al., "Contributions of altimetry and argo to non-closure of the global mean sea level budget since 2016," *Geophys. Res. Lett.*, vol. 48, no. 14, 2021, Art. no. e2021GL092824, doi: 10.1029/2021gl092824.

[24] J. F. Crétaux et al., "Lake volume monitoring from space," *Surv. Geophys.*, vol. 37, no. 2, pp. 269–305, 2016, doi: 10.1007/s10712-016-9362-6.

[25] B. D. Loomis, K. E. Rachlin, and S. B. Luthcke, "Improved earth oblateness rate reveals increased ice sheet losses and mass-driven sea level rise," *Geophys. Res. Lett.*, vol. 46, no. 12, pp. 6910–6917, 2019, doi: 10.1029/2019gl082929.

[26] F. W. Landerer, "Monthly estimates of degree-1 (geocenter) gravity coefficients, generated from GRACE (04-2002–06/2017) and GRACE-FO (06/2018 onward) RL06 solutions," GRACE Technical Note 13, NASA Jet Propulsion Laboratory, 2019. [Online]. Available: https://podaac-tools.jpl.nasa.gov/drive/files/allData/grace/docs/TN-13_GEOC_CSR_RL06.txt

[27] W. R. Peltier, D. F. Argus, and R. Drummond, "Comment on 'an assessment of the ICE-6G_C (VM5a) glacial isostatic adjustment model' by Purcell et al," *J. Geophys. Res. Solid Earth*, vol. 123, no. 2, pp. 2019–2028, 2018, doi: 10.1002/2016jb013844.

[28] J. L. Chen et al., "Long-term Caspian Sea level change," *Geophys. Res. Lett.*, vol. 44, no. 13, pp. 6993–7001, 2017, doi: 10.1002/2017gl073958.

[29] J. L. Chen, C. R. Wilson, and B. D. Tapley, "Interannual variability of Greenland ice losses from satellite gravimetry," *J. Geophys. Res.*, vol. 116, no. B7, p. B07406, 2011, doi: 10.1029/2010jb007789.

[30] J. L. Chen, C. R. Wilson, J. S. Famiglietti, and M. Rodell, "Attenuation effect on seasonal basin-scale water storage changes from GRACE time-variable gravity," *J. Geodesy*, vol. 81, no. 4, pp. 237–245, 2006, doi: 10.1007/s00190-006-0104-2.

[31] J. Wahr, M. Molenaar, and F. Bryan, "Time variability of the Earth's gravity field: Hydrological and oceanic effects and their possible detection using GRACE," *J. Geophys. Res. Solid Earth*, vol. 103, no. B12, pp. 30205–30229, 1998, doi: 10.1029/98jb02844.

[32] M. Rodell et al., "The global land data assimilation system," *Bull. Amer. Meteorological Soc.*, vol. 85, no. 3, pp. 381–394, 2004, doi: 10.1175/bams-85-3-381.

[33] H. Save, S. Bettadpur, and B. D. Tapley, "High-resolution CSR GRACE RL05 Mascons," *J. Geophys. Res. Solid Earth*, vol. 121, no. 10, pp. 7547–7569, 2016, doi: 10.1002/2016jb013007.

[34] H. Save, "CSR GRACE and GRACE-FO RL06 Mascon solutions v02," Center Space Res., Univ. Texas, Austin, USA, 2020, doi: 10.15781/cgq9-nh24.
[35] D. N. Wiese, F. W. Landerer, and M. M. Watkins, "Quantifying and reducing leakage errors in the JPL RL05M GRACE Mascon solution," *Water Resour. Res.*, vol. 52, no. 9, pp. 7490–7502, 2016, doi: 10.1002/2016wr019344.
[36] M. M. Watkins, D. N. Wiese, D.-N. Yuan, C. Boening, and F. W. Landerer, "Improved methods for observing Earth's time variable mass distribution with GRACE using spherical cap mascons," *J. Geophys. Res. Solid Earth*, vol. 120, no. 4, pp. 2648–2671, 2015, doi: 10.1002/2014jb011547.
[37] B. D. Loomis, S. B. Luthcke, and T. J. Sabaka, "Regularization and error characterization of GRACE mascons," *J. Geodesy*, vol. 93, no. 9, pp. 1381–1398, Sep. 2019, doi: 10.1007/s00190-019-01252-y.
[38] D. Roemmich and B. Owens, "The argo project: Global ocean observations for understanding and prediction of climate variability," *Oceanography*, vol. 13, no. 2, pp. 45–50, 2000, doi: 10.5670/oceanog.2000.33.
[39] S. Levitus et al., "World ocean heat content and thermosteric sea level change (0–2000 m), 1955–2010," *Geophys. Res. Lett.*, vol. 39, no. 10, p. L10603, 2012, doi: 10.1029/2012gl051106.
[40] Y. H. Zhou and D. W. Z., "Monte Carlo simulation tests of correlation significance levels," *Acta Geodaetica Cartographica Sinica*, vol. 28, no. 4, pp. 313–318, 1999.
[41] P. Ditmar, "How to quantify the accuracy of mass anomaly time-series based on GRACE data in the absence of knowledge about true signal?," *J. Geodesy*, vol. 96, no. 8, pp. 1–22, 2022, doi: 10.1007/s00190-022-01640-x.
[42] J. Chen, A. Cazenave, S.-Y. Wang, and J. Li, "Caspian Sea level change observed by satellite altimetry," *Remote Sens.*, vol. 15, no. 3, pp. 1–22, 2023, doi: 10.3390/rs15030703.
[43] L. Wang, C. Chen, M. Thomas, M. K. Kaban, A. Güntner, and J. Du, "Increased water storage of Lake Qinghai during 2004–2012 from GRACE data, hydrological models, radar altimetry and in situ measurements," *Geophys. J. Int.*, vol. 212, no. 1, pp. 679–693, 2018.

Jianli Chen received the Ph.D. degree in geophysics from the University of Texas at Austin, Austin, TX, USA, in 1998.

He is a Strategic Hiring Scheme (SHS) Professor with the Department of Land Surveying and Geo-Informatics, The Hong Kong Polytechnic University, Hong Kong, China. His research interests include space geodesy and climate change.

Dr. Chen was the recipient of 2005 Presidential Early Career Awards for Scientists and Engineers. He is a fellow of the International Association of Geodesy, has severed as the chair of the IERS Special Bureau for Hydrology since 2004, and co-chair/chair of the IAG Commission 3.3 (Earth Rotation and Geophysical Fluids) since 2012.

Clark Wilson received the Ph.D. degree in earth sciences from the Scripps Institution of Oceanography, La Jolla, CA, USA, in 1975.

He has served twice as Geological Sciences Department Chairman (1990–1994 and 2004-2007). He has served on the Board of Directors with the International Earth Rotation and Reference Frame Service and on the Board of UNAVCO, Inc. as Corporate Treasurer. He is currently a Professor Emeritus with the University of Texas at Austin, Austin, TX, USA. His research interests include geophysics and space geodesy.

Ki-Weon Seo received the Ph.D. degree in geophysics from the University of Texas at Austin, Austin, TX, USA, in 2005.

He is a Professor with the Department of Earth Science Education, Seoul National University, Seoul, South Korea. His research interests include geophysics and space geodesy.

Anny Cazenave received the Ph.D. degree in geophysics from the Université Paul Sabatier, Toulouse, France, in 1975.

She was Director for Earth sciences with the International Space Science Institute, Bern, Switzerland. She is Emeritus Scientist with the "Laboratoire d'Etudes en Géophysique et Océanographie Spatiales," Toulouse. She served as lead author of the IPCC (Intergovernmental Panel on Climate Change) Working Group I (4th and 5th Assessment Reports). Her research interests include the applications of space techniques to Earth sciences.

Dr. Cazenave is a member of the French Academy of Sciences and foreign member of the NAS, the Royal Society, and Indian and Belgian academies of sciences.

Songyun Wang received the Ph.D. degree in geophysics from the Shanghai Astronomical Observatory, Chinese Academy of Sciences, Beijing, China, in 2018.

He is a Research Associate with the Center for Space Research, University of Texas at Austin, Austin, TX, USA. His research interests include geophysics and space geodesy.

Jin Li received the Ph.D. degree in geophysics from the Wuhan University, Wuhan, China, in 2011.

He is a Professor with the Shanghai Astronomical Observatory, Chinese Academy of Sciences, Shanghai, China. His research interests include geophysics and space geodesy.

Yufeng Nie received the Ph.D. degree in geodesy from the Tongji University, Shanghai, China, in 2023.

He is a postdoctoral fellow with the Department of Land Surveying and Geo-Informatics, Hong Kong Polytechnic University, Hong Kong, China. His research interests include satellite gravimetry and its applications.